BIOCHEMISTRY
including biophysical chemistry & molecular biology

ARTICLE

pubs.acs.org/biochemistry

Biochemical Characterization of Human SET and MYND Domain-Containing Protein 2 Methyltransferase

Jiaquan Wu,[*,†] Tony Cheung,[†,§] Christie Grande,[†,§] Andrew D. Ferguson,[‡] Xiahui Zhu,[†] Kelly Theriault,[†] Erin Code,[†] Cynthia Birr,[†] Nick Keen,[†] and Huawei Chen[*,†]

[†]Oncology Innovative Medicines Unit, AstraZeneca Pharmaceuticals, 35 Gatehouse Drive, Waltham, Massachusetts 02451, United States

[‡]DECS Structural Chemistry, AstraZeneca Pharmaceuticals, 35 Gatehouse Drive, Waltham, Massachusetts 02451, United States

ABSTRACT: SET and MYND domain-containing protein 2 (SMYD2) is a protein lysine methyltransferase that catalyzes the transfer of methyl groups from *S*-adenosylmethionine (AdoMet) to acceptor lysine residues on histones and other proteins. To understand the kinetic mechanism and the function of individual domains, human SMYD2 was overexpressed, purified, and characterized. Substrate specificity and product analysis studies established SMYD2 as a monomethyltransferase that prefers nonmethylated p53 peptide substrate. Steady-state kinetic and product inhibition studies showed that SMYD2 operates via a rapid equilibrium random Bi Bi mechanism at a rate of $0.048 \pm 0.001\ s^{-1}$, with K_Ms for AdoMet and the p53 peptide of $0.031 \pm 0.01\ \mu M$ and $0.68 \pm 0.22\ \mu M$, respectively. Metal analyses revealed that SMYD2 contains three tightly bound zinc ions that are important for maintaining the structural integrity and catalytic activity of SMYD2. Catalytic activity was also shown to be dependent on the GxG motif in the S-sequence of the split SET domain, as a G18A/G20A double mutant and a sequence deletion within the conserved motif impaired AdoMet binding and significantly decreased enzymatic activity. The functional importance of other SMYD2 domains including the MYND domain, the cysteine-rich post-SET domain, and the C-terminal domain (CTD), were also investigated. Taken together, these results demonstrated the functional importance of distinct domains in the SMYD family of proteins and further advanced our understanding of the catalytic mechanism of this family.

Reversible methylation of lysine residues on histones is an important mechanism in epigenetic gene regulation.[1−5] More recent studies have shown that the methylation and demethylation of lysine residues, as demonstrated with nonhistone proteins such as p53,[6,7] pRB,[8] E2F1,[9] RelA,[10,11] VEGFR,[12] and DNMT1[13] also serve as a molecular switch for other cellular events such as signal transduction.[5] It is therefore not surprising to see increasing reports that link deregulation of methylation homeostasis to human diseases, especially cancers.

These reversible post-translational modifications are driven by protein lysine methyltranferases (PKMTs) and demethylases. PKMTs catalyze the transfer of methyl groups from the cosubstrate *S*-adenosylmethionine (AdoMet or SAM) to the ε-amine of an acceptor lysine residue on histone and nonhistone protein substrates. Acceptor lysine residues can be mono-, di-, or trimethylated, and discrete methylation states are specifically recognized by effector molecules, leading to differential functional consequences.[14]

There are about 50 PKMTs in the human genome. With the exception of Dot1L, all PKMTs contain a conserved SET (Suppressor of variegation, Enhancer of zeste, Trithorax) domain where several conserved sequence motifs (I−IV) are clustered together in the tertiary structure, critical for substrate binding and catalysis.[15] In addition to the SET domain, the catalytic activity of PKMTs often requires two flanking domains: the N-terminal pre-SET domain and the C-terminal post-SET domain. However, these domains vary among PKMTs, and conservation among the subgroup is used as the basis for subfamily classification.[15]

The SMYD protein family is a subfamily of PKMTs that contain five members, SMYD1−5, which all share a similar domain arrangement. Primary sequence analysis shows that the SMYD proteins contain an S-sequence (N-terminal portion of the split SET domain), a MYND (Myeloid, Nervy and DEAF-1) domain, a SET-I (inserted domain), a split SET domain (C-terminal portion of the SET domain), a post-SET domain, and an extended C-terminal domain (CTD) (Figure 1A).[16] The MYND domain is a zinc finger motif that mediates protein−protein interactions. Abu-Farha et al. have shown that SMYD2 utilizes its MYND domain to interact with proline-rich proteins such as EPB41L3.[17] The split SET domain of SMYD proteins contains three distinct functional regions: the GxG, NHSC, and GEE motifs. Deletion of either the NHSC or GEE motifs abolished the methyltransferase activity of SMYD2.[17] Unexpectedly, removing the GxG motif of SMYD3, a close analogue of SMYD2, significantly enhanced SMYD3 enzymatic activity.[18] The post-SET domain of SMYD2 contains a cysteine-rich motif that is similar to several other PKMTs, including Dim-5 and G9a. The crystal structures of these PKMTs showed that a single zinc ion is coordinated by three cysteine residues from the post-SET domain and a fourth cysteine residue from the SET core domain.[19,20] Little is known about the function of the CTD of SMYD proteins.

Received: May 10, 2011
Revised: June 15, 2011
Published: June 16, 2011

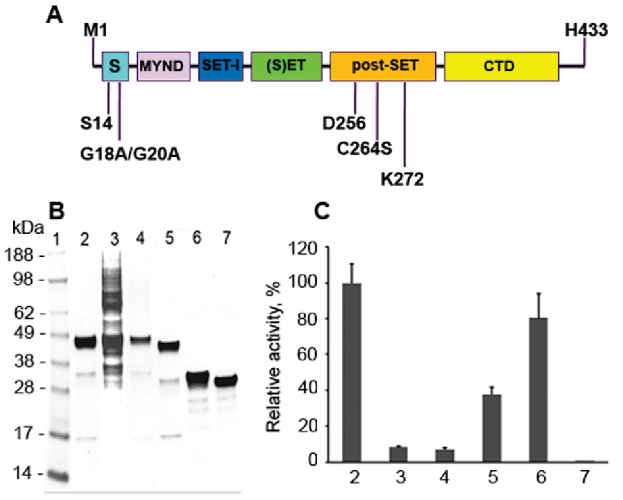

Figure 1. Expression, purification, and methyltransferase activity of SMYD2 proteins. (A) Schematic representation of SMYD2 domain structure. Labeled residues indicate the locations for truncation and mutations made shown in (B) and (C). (B) SDS-PAGE gel of wild-type and mutant proteins. Lane 1, MW markers; lanes 2−7, wild-type, C264S, G18A/G20A, SMYD2-dN1(S14−H433), SMYD2-dC2 (M1−K272), and SMYD2-dC3 (M1−D256). (C) Methyltransferase activity of SMYD2 protein. Reactions were performed using 275 nM of protein in TDT buffer with 0.5 μM ^{3}H-AdoMet and 2 μM recombinant histone H3.2 at room temperature for 2 h, and products were quantified using a SPA binding assay. Each data point is the average of at least three replicates, and the bars represent the standard deviations.

Mechanistically, most of the AdoMet-dependent protein methyltransferases utilize sequential Bi Bi kinetic mechanisms in which both AdoMet and the protein substrate are bound before the methyl transfer reaction occurs. This was shown to be the case for G9a and PRMT1, where kinetic studies indicated both enzymes catalyze histone H3 (G9a) and H4 (PRMT1) methylation via a random sequential Bi Bi mechanism.[21,22] In contrast, isoprenylcysteine carboxylmethyltransferase (ICMT), an AdoMet-dependent cysteine protein methyltransferase that catalyzes the last step of the post-translational modification of Ras proteins, uses an ordered sequential Bi Bi mechanism whereby AdoMet binds to ICMT prior to the protein substrate and AdoHcy is released after protein substrate methylation.[23] The catalytic mechanism of SMYD2 remains to be established.

SMYD2 was first identified as a histone H3 Lys36 (H3K36) specific methyltransferase.[16] Subsequent proteomic and genomic studies suggested that SMYD2 could dimethylate histone H3K4.[17] Aside from histone H3, SMYD2 was recently reported to monomethylate tumor suppressor proteins p53[7] and pRb[8] at K370 and K860, respectively, to impair the tumor suppressor activities of these proteins. Recent studies indicated that the genomic region where the SMYD2 gene resides, 1q32, is frequently amplified in various human solid tumors, and that overexpression of SMYD2 was able to drive proliferation of esophageal squamous cell carcinoma (ESCC) cells and predict a poor outcome in ESCC patients.[24,25] Another SMYD family member, SMYD3, has been shown to play a key role in oncogenesis in multiple solid tumors.[26] Here, we present the overexpression, purification, and enzymatic characterization of recombinant human SMYD2. We investigated the optimal catalytic conditions and substrate and product specificity. The functional roles of the four distinct SMYD2 domains in substrate binding and catalysis were also established. Finally, the kinetic mechanism of the SMYD2-catalyzed methylation reaction and the inhibition mechanism of the AdoHcy product were also studied.

EXPERIMENTAL PROCEDURES

Materials. All reagents were purchased from Sigma-Aldrich unless specified. A plasmid harboring full-length human SMYD2 gene was purchased from GeneCopoiea (Rockville, MD). Tritium-labeled *S*-adenosylmethionine (^{3}H-AdoMet) was purchased from PerkinElmer (Waltham, MA). The p53 peptide substrate (Biotin-aminohexanoyl-GSRAHSSHLKSKKGQSTSRH, termed as p53K370Me$_0$) and its methylated counterpart were synthesized by 21st Century Biochemicals (Marlboro, MA). The p53 protein was expressed and purified from *Sf*9 cells. Histones H2B, H3.2, and H4 were purchased from New England Biolabs (Ipswich, MA). The histone H3 peptide (residues 1−45) was a generous gift from 21st Century Biochemicals. All other histone peptides were purchased from AnaSpec (Fremont, CA).

Molecular Biology. A cDNA fragment corresponding to residues 1−433 of human SMYD2 was PCR amplified from GeneCopoiea plasmid EX−W0719-B01 using the following primers: 5′-AGGGCGCCATGGATCCGATGAGGGCCGAGGGCCTCGGCGGC-3′ (sense strand) and 5′−TACCGCATGCCTCGAG TCAGTGGCTTTCAATTTCCTGTTT-3′ (antisense strand). A baculovirus expression vector was constructed by subcloning a *Bam*HI/XhoI digested fragment containing full-length SMYD2 with an N-terminal His$_6$-tag into the baculovirus transfer vector pFastBacHTa (Invitrogen). Site-directed mutagenesis was performed on this plasmid to generate mutants using the following primers: G18A/G20A double mutant, 5′-CTGCAGCCCGGGCAAAGCAAGAGCGCTGCGGGCTCTGCAG-3′ (sense strand) and 5′-CTGCAGAGCCCGCAGCGCTCTTGCTTTGCCCGGGCTGCAG-3′ (antisense strand); C52S, 5′-CGGGGCAACCACTCAGAGTACTGCTTCAC-3′ (sense strand) and 5′-GTGAAGCAGTACTCTGAGTGGTTGCCCCG-3′ (antisense strand); C90S, 5′-GCACAAGCTGGAATCTTCTCCCATGGTTG-3′ (sense strand) and 5′-CAACCATGGGAGAAGATTCCAGCTTGTGC-3′ (antisense strand); Y217F, 5′-GTCATTGTGACCTTCAAAGGGACCCTGG-3′ (sense strand) and 5′-CCAGGGTCCCTTTGAAGGTCACAATGAC-3′ (antisense strand); C264S, 5′-CTTTACCTGTGAGAGCCAGGAGTGTACC-3′ (sense strand) and 5′-GGTACACTCCTGGCTCTCACAGGTAAAG-3′ (antisense strand). Truncation constructs were generated by PCR amplification using the full-length wild-type template and subcloning into baculovirus vectors using the following primers: C13−H433 (SMYD2-dN1), 5′−GGATCCGATGTGCAGCCCGGGCAAAGGCCGGGGGCT-3′ (sense strand) and 5′−CTCGAGTCAGTGGCTTTCAATTTCCTGTTTGATCTCGGA−3′ (antisense strand). Additionally, DNA for M1-K272 (SMYD2-dC2) and M1-D256 (SMYD2-dC3) were synthesized by GENEART (Regensburg, Germany). All sequences were verified by automated DNA sequencing.

Recombinant SMYD2. *Spodoptera frugiperda* (*Sf*21) cells were infected with recombinant baculoviruses using a multiplicity of infection of 1. Infected insect cells were harvested 48 h postinfection by centrifugation and stored at −80 °C. Cell pellets were resuspended in 25 mM Tris lysis buffer and lysed hypotonically. The cell lysate was centrifuged at 10000 rpm for 45 min. The clarified cell lysate was incubated with Ni-NTA agarose

beads (Qiagen) for 1−2 h at 4 °C. The Ni-NTA beads were collected by centrifugation at 3000 rpm for 5 min, washed with Tris buffer, and eluted with Tris buffer containing 0.2 M imidazole. SMYD2-containing fractions were pooled and applied to a Superdex200 column equilibrated with Tris running buffer. Purified SMYD2 fractions were pooled, concentrated, snap-frozen in liquid nitrogen, and stored at −80 °C.

ICP-MS Assay. Metal analysis was performed as described previously[27] using inductively coupled plasma mass spectrometry (ICP-MS) on a VG PlasmaQuad 3 ICP instrument (Elemental Analysis Inc. Lexington, KY). This method provides information on the identity and quantity of metal contained in protein samples. For zinc quantification, a buffer only sample was run prior to each protein sample as background control. Data for each protein sample was the average of at least three samples.

PAR/PMB Assay. The zinc content of SMYD2 was analyzed with a spectrophotometric assay based on the absorbance change of 4-(2-pyridylazo)-resorcinol (PAR)[27,28] following its complexation with zinc when released from SMYD2 by *p*-(hydroxymercuri)-benzoic acid (PMB) treatment.[29,30] Briefly, protein aliquots were mixed with increasing concentrations of PMB at room temperature in 50 mM Tris (pH 9). Following a 90 min incubation, a PAR solution was added to each SMYD2/PMB mixture, and the samples were incubated at room temperature for 30 min. Sample absorbance was recorded at 500 nm using a SpectraMax PLUS spectrophotometer (Molecular Devices Corp., Sunnyvale, CA). The concentration of zinc in each sample was determined by using a zinc standard curve obtained with a zinc ICP standard (Sigma).

Methyltransferase Activity Assays. Methyltransferase activity was evaluated using radiometric assays, including a filter binding assay for kinetic characterization and a scintillation proximity assay (SPA) for biochemical characterization. Specifically, the filter binding assay was performed at room temperature in TDT buffer (50 mM Tris pH 9, 2 mM DTT, and 0.02% Tween 20). Then 60 μL reaction mixtures containing SMYD2, varied concentrations of ^{3}H-AdoMet, and the p53K370Me$_0$ substrate (unless specifically mentioned) were incubated in a 96-well reaction plate. Fifty microliter aliquots were then transferred to a 96-well MultiScreen HTS FB plate (Millipore Corp., MA) with 50 μL of 2% TCA, incubated for 10 min, and dried under vacuum. The dried reactions were washed five times each with 200 μL of 2% TCA and 100% methanol, allowed to dry, and then resuspended with 100 μL of Microscint solution (PerkinElmer) and read with a TopCount 384 radioactivity counter (PerkinElmer). The SPA assay reactions were identical to those described for the filter binding assay except for the use of 384-well low volume plates (Thermo Fisher Sci. Inc., NH) and a reduced reaction volume of 12 μL. The reactions were quenched by the addition of AdoHcy and Streptavidin-coated SPA beads (GE Life Sci., MA), incubated overnight, and read with a TopCount 384 radioactivity counter.

Steady-State Kinetics. Bisubstrate kinetic analyses were performed using the filter binding assay described above. All reactions contained 5 nM SMYD2 and varied concentrations of substrates, and were quenched for product quantification after a 10 min incubation at room temperature. Under such conditions, the SMYD2 reaction time-courses were linear up to 40 min (data not shown). Initial velocities were determined for SMYD2 catalyzed reactions with varied concentrations of ^{3}H-AdoMet and the p53K370Me$_0$ substrate. Each reaction was repeated a minimum of three times. Initial velocity data were fitted to the following equations[31] using GraFit 5.0 (Erithacus Software).

For an ordered sequential mechanism:

$$v = \frac{V_{max} \cdot [A] \cdot [B]}{K_A K_{Bm} + K_{Bm}[A] + K_{Am}[B] + [A][B]} \quad (1)$$

For a random sequential mechanism:

$$v = \frac{V_{max} \cdot [A] \cdot [B]}{\alpha K_A K_B + \alpha K_B [A] + \alpha K_A [B] + [A][B]} \quad (2)$$

For a Ping-Pong mechanism:

$$v = \frac{V_{max} \cdot [A] \cdot [B]}{K_{Am}[B] + K_{Bm}[A] + [A][B]} \quad (3)$$

The equation(s) that most accurately described the initial velocity data was identified by nonlinear regression analysis and was used to calculate steady-state kinetic parameters.

Product Inhibition. The inhibition modes of the SMYD2 catalyzed reaction product AdoHcy were evaluated using a filter binding assay. Initial reaction velocities were determined using varied concentrations of one substrate and one product and a fixed concentration of the other substrate. Data were fitted to the following equations with GraFit 5.0.

For competitive inhibition:

$$v = \frac{V_{max} \cdot [S]}{[S] + K_m \cdot (1 + [I]/K_{is})} \quad (4)$$

For noncompetitive inhibition:

$$v = \frac{V_{max} \cdot [S]}{(K_m \cdot (1 + [I]/K_{is})) + [S] \cdot (1 + [I]/K_{ii})} \quad (5)$$

For uncompetitive inhibition:

$$v = \frac{V_{max} \cdot [S]}{K_m [S] \cdot (1 + [I]/K_{ii})} \quad (6)$$

Nonlinear least-squares regression analysis was used to determine which equation accurately described the experimental data.

RESULTS AND DISCUSSION

Expression, Purification, and Activity of SMYD2. Recombinant SMYD2 expressed and purified from bacteria showed only moderate enzymatic activity (data not shown). To improve the yield and activity of the recombinant protein, the SMYD2 gene was subcloned into a baculovirus expression vector and expressed in *Sf*21 cells (Figure 1B). Wild-type SMYD2 with an N-terminal His$_6$-tag expressed in insect cells has at least 6-fold higher specific methyltransferase activity compared to the bacterial protein when using full-length histone H3 as the receptor substrate (data not shown). MALDI-TOF mass spectrometry showed that the molecular mass of the purified protein was 53.0 ± 0.1 kDa, consistent with the calculated molecular mass of 53.1 kDa. Several mutants were made and purified to interrogate the functional roles of several distinct domains in the SMYD2 protein as depicted in Figure 1A. We also attempted to prepare three cysteine mutants (C52S, C90S, and C264S) to study the functional role of zinc binding, but only succeeded in obtaining the C264S mutant.

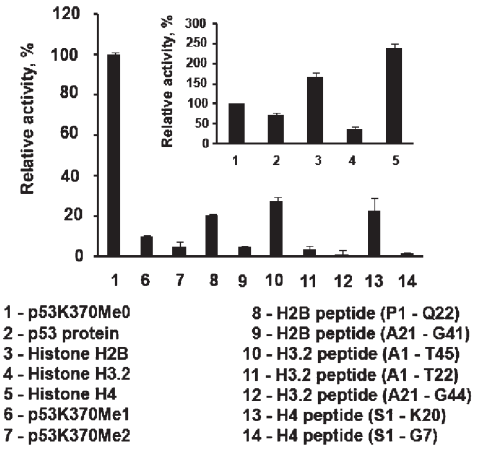

Figure 2. Substrate specificity of SMYD2. Specific activity of SMYD2 was determined using the filter binding assay described in Experimental Procedures. SMYD2 was used at 5 nM (when proteins were used as substrate) or 125 nM (when peptides were used as substrate), and substrates (protein, peptide, and AdoMet) were used at 1 μM. Reactions were allowed to progress at room temperature for 1 h before quenching. Raw data were normalized against p53 peptide activity. Error bars represent the standard deviation of triplicate samples for each reaction.

Substrate and Product Specificity of SMYD2. It has been shown that SMYD2 can methylate K36 and/or K4 of histone H3, K370 of p53, and K860 of pRb, using immunoprecipitated material. Here, we extend this work by using recombinant SMYD2 protein and characterizing its activity against a panel of potential substrates, including full-length H2B, H3.2, H4, and p53 proteins, and synthetic peptides derived from these proteins, for identifying a suitable substrate for high throughput screening assay development.

All full-length proteins were methylated by SMYD2 in a radiometric assay. H2B and H4 are more efficient substrates with 3- to 5-fold higher specific activity compared to H3 (Figure 2, insert). These findings raise interesting questions of whether H2B and H4 are endogenous substrates for SMYD2 in vivo and what are the biological consequences of SMYD2-mediated methylation on these histone proteins. Among the peptides tested, the p53K370Me$_0$ (G361-H380) peptide had the highest specific activity (Figure 2).

Additional experiments were carried out to assess substrate and product specificity. While the nonmethylated p53K370Me$_0$ peptide showed robust activity, the monomethylated p53K370Me$_1$ peptide only showed marginal activity and the dimethylated p53K370Me$_2$ was completely inactive, strongly indicating that SMYD2 is a monomethyltransferase that prefers nonmethylated p53 as its substrate. We confirmed the product specificity by analyzing the degree of methylation using LC-MS. The dominant turnover product (~80%) was still p53K370Me$_1$ after prolonged incubation of p53K370Me$_0$ with excess amounts of SMYD2 enzyme and AdoMet cosubstrate. Previous reports suggested that SMYD2 dimethylated H3K4[17] and H3K36[16] when specific antibodies were used for product characterization. Although the reliability of an antibody-based readout depends entirely on the quality of antibody reagents and the degree of validation, it is possible that SMYD2 product specificity is context dependent such that auxiliary proteins and the local microenvironment may guide the degree of methylation.

Methylation of histone H3 appears to be sequence dependent. Full-length H3 was an efficient substrate for SMYD2 (~40% specific activity compared to p53K370Me$_0$). While the long N-terminal peptide (A1-T45) still showed reasonable activity, the two shorter H3 peptides (A1-A21, and A21 -G44) were not active. Methylation of both H2B and H4 appeared to occur at the N-termini, as SMYD2 methylated the N-terminal peptides of both proteins but not the C-terminal peptides (Figure 2). More work is needed to establish the site(s) and degree of methylation.

Optimal Catalytic Conditions for SMYD2. *pH Dependence.* PKMTs lack an active site residue that functions as a general base to deprotonate the acceptor lysine residue for nucleophilic attack of the C−S bond of AdoMet. The lysine-binding channels of most PKMTs are negatively charged, and these electrostatic states may facilitate proton removal. Although the calculated pK_a of the amine group of lysine is ~10, when positioned within the lysine-binding channel, the pK_a of the acceptor lysine amine could decrease to ~8 to facilitate the deprotonation reaction.[32] To test this hypothesis, we evaluated the specific activity of SMYD2 across a broad pH range. SMYD2 showed minimal activity in HEPES buffer with pH values below 7.5 (Figure 3A) and moderate activity in Tris buffer from pH 7.5 to pH 8.5. SMYD2 activity increased dramatically from pH 8.5 to pH 9.2, peaking at pH 9.1. We also determined the K_M values for AdoMet at several different pH conditions and observed no changes in the AdoMet K_M (data not shown), suggesting that the pH effect on SMYD2 catalytic efficiency is mainly a k_{cat} driven effect. Dirk et. al made a similar observation with SET7/9 PKMT, where the k_{cat} of SET7/9 was increased by 7-fold with an increase in pH from 7.5 to 9.5, while the K_Ms of both AdoMet and H3 remained the same.[33] The pH profile of SMYD2 activity is consistent with the notion that solvent basicity may contribute to the deprotonation of the ε-amine group of K370 on the p53 peptide substrate.

Other Condition Factors. SMYD2 activity was sensitive to ionic strength, with optimal activity observed under low ionic strength (Figure 3B). The methyltransferase activity of SMYD2 was also sensitive to detergent. Including a trace amount of detergent was sufficient to stimulate maximal activity. For example, 0.001% (w/v) Tween-20 enhanced SMYD2 methyltransferase activity by more than 4-fold (Figure 3C). Small amounts of Tween-20 presumably could stabilize SMYD2 or prevent nonspecific binding of proteins to plastic surfaces.

SMYD2 contains three cysteine-rich motifs that could presumably coordinate zinc ions, implying that thiol-based reductants such as DTT could negatively affect methyltransferase activity. We evaluated the effect of DTT and TCEP (a nonthiol reductant) on SMYD2 activity. Surprisingly, TCEP suppressed activity in a dose-dependent manner (Figure 3D), whereas DTT did not. The temperature-dependence activity profile of SMDY2 (Figure 3E) resembles those of other PKMTs, especially G9a[21] and Dim-5.[34] Under these experimental conditions, SMYD2 had maximal activity at ~32 °C, with activity rapidly dropping at temperatures above 37 °C.

Metal Analysis. When we began this study, there were no reports regarding the identity and the stoichiometry of metal ions in SMYD proteins. Protein sequence analysis indicated the presence of a MYND domain, which contains a putative non-DNA binding zinc-finger that normally binds two zinc ions, and a cysteine-rich post-SET domain that likely coordinates an additional zinc ion. The zinc binding stoichiometry was initially analyzed using a PMB/PAR spectrophotometric assay. The organomercurial compound PMB has been shown to trap the cysteine thiol group of proteins by mercuration, thereby releasing bound zinc.[35] The addition of PMB to SMYD2 released zinc, which was chelated by PAR, producing an orange-colored complex (Figure 4, left panel). The absorbance at 500 nm was

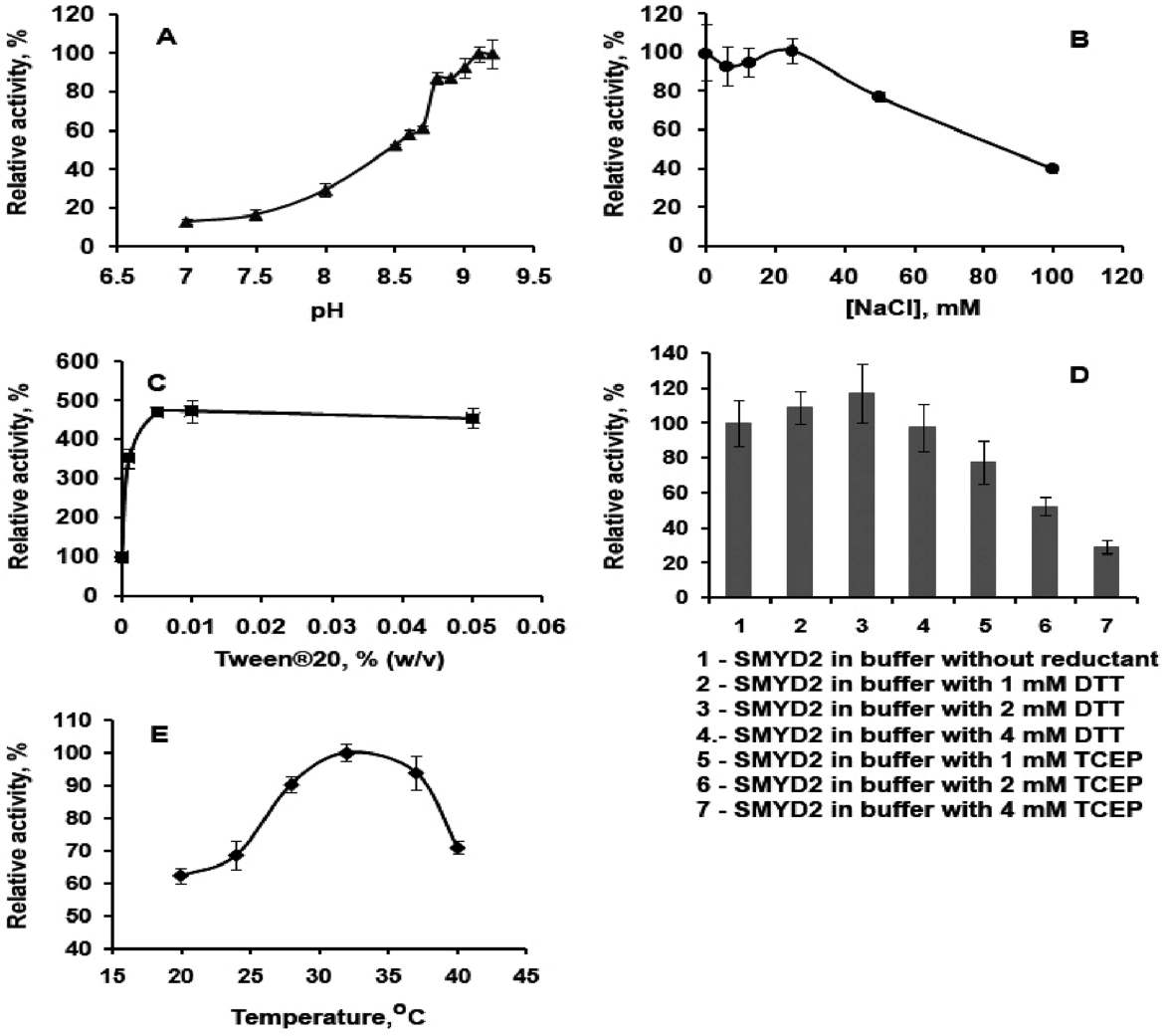

Figure 3. Biochemical properties of SMYD2. Reactions were conducted by using 5 nM SMYD2, 1 μM ^{3}H-AdoMet, and 1 μM p53K370Me$_0$ peptide, in HEPES or Tris buffer, and were detected using the SPA assay described in Experimental Procedures. Each data point is an average of triplicates and the bars represent the standard deviation of triplicates. (A) pH Dependence of SMYD2 activity; (B) ionic strength dependence of SMYD2 activity; (C) detergent concentration dependence of SMYD2 activity; (D) reductant concentration dependence of SMYD2 activity; (E) temperature dependence of SMYD2 activity.

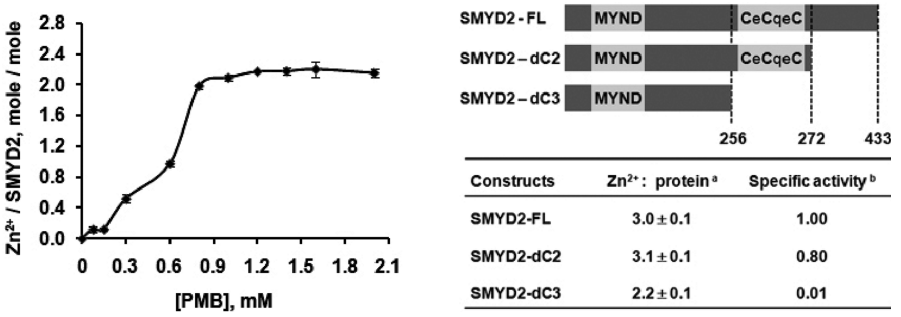

Constructs	Zn^{2+} : protein [a]	Specific activity [b]
SMYD2-FL	3.0 ± 0.1	1.00
SMYD2-dC2	3.1 ± 0.1	0.80
SMYD2-dC3	2.2 ± 0.1	0.01

Figure 4. Zinc content analyses. (left) PMB titration curve. SMYD2 was incubated with PMB and PAR, and zinc released from the protein was quantitated as described in Experimental Procedures. Each data point is an average of triplicates and the bars represent the standard deviation of triplicates. Right panel shows the constructs that were used in the ICP-MS analysis. The MYND and post-SET domain cysteine-rich motifs (top) and the associated zinc content and relative activities (bottom) are shown. Table footnote *a*, zinc-to-protein binding stoichiometry as determined by ICP-MS spectrometry; table footnote *b*, specific activity was measured using the filter binding assay described in Experimental Procedures. Specific activity is expressed as the fraction of wild-type SMYD2 activity.

measured, and the zinc concentration was determined by comparison to a standard curve prepared under identical conditions. Then 2.2 zinc ions per SMYD2 molecule were released under saturating PMB concentrations (Figure 4, left panel). Interestingly, the

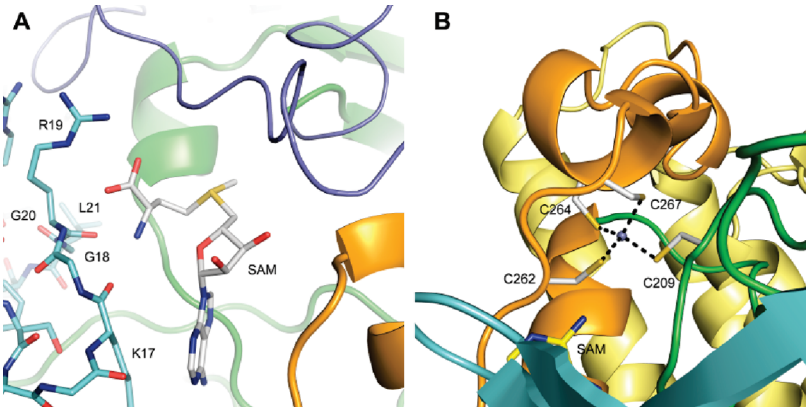

Figure 5. Crystal structure of SMYD2.[40] (A) AdoMet binding site. The protein backbone is shown in ribbon representation with the S-sequence domain colored cyan, SET-I domain colored blue, core SET domain colored green, the post-SET domain colored orange, and the C-terminal domain colored yellow. The cosubstrate AdoMet is shown in stick representation with white carbon atoms, blue nitrogen atoms, red oxygen atoms, and orange sulfur atoms. (B) Post-SET domain zinc binding site. The protein backbone is shown in ribbon representation with the S-sequence domain colored cyan, core SET domain colored green, the post-SET domain colored orange, and the C-terminal domain colored yellow. Zinc ions are shown as purple spheres. Dashed lines indicate the coordination of the zinc ion by residues C262, C264, and C267 from the post-SET domain and residue C209 from the core SET domain.

stoichiometry increased to 2.7 for the C-terminal truncation mutant SMYD2-dC2 (residues 1−272) that contains all four post-SET domain cysteine residues that potentially coordinate a zinc ion, implying that SMYD2 likely contains three zinc ions and that truncating the C-terminus may facilitate the release of zinc ions. We then used quadrupole ICP-MS spectrometry to unambiguously identify bound zinc ions in the recombinant SMYD2 while further confirming the stoichiometry (Figure 4, right panel). Removal of the post-SET domain in SMYD2-dC3 resulted in the reduction of one zinc ion, whereas a stoichiometry of three was observed in the full-length SMYD2 and the CTD-truncated SMYD-dC2. The apparent discrepancy between the zinc stoichiometry determined by the PMB/PAR assay and the ICP-MS assay could be due to the incomplete mercuration of SMYD2 cysteine residues by PMB, while in the ICP-MS assay, the protein was fully denatured and all zinc ions were released for quantitation.

Functional Analysis of the Conserved GxG Motif in the Split SET Domain. The GxG motif is well conserved in SET-domain containing PKMTs. In the SMYD family, this motif is found within the S-sequence, which is the N-terminal part of the SET domain that is split by the MYND and SET-I domains (Figure 1A). The GxG motif is believed to be important for the binding of cosubstrate AdoMet. Surprisingly, it was reported that the S-sequence of SMYD3 had an inhibitory effect on SMYD3 activity and that its removal or perturbation enhanced activity.[18] As SMYD2 and SMYD3 share a good degree of sequence similarity (~50%) and have identical domain organization, we assessed the functional role of this region by characterizing the activities of a series of deletions and point mutations of SMYD2 (Figure 1). A double mutant (G18A/G20A) (Figure 1B, lane 4) within the GxG motif showed significantly decreased enzymatic activity (Figure 1C, column 4) by impairing AdoMet binding. The K_M for the G18A/G20A mutant was 0.60 ± 0.33 μM, about 20-fold higher than wild-type SMYD2 (0.031 ± 0.010 μM). Consistent with the notion that the GxG motif is mainly involved in AdoMet binding in PKMTs, the V_{max} value of the mutant protein remained unchanged (data not shown). An alternative GxG patch (G5/G7) in the S-sequence exists, but mutating these residues to alanine did not affect the specific enzymatic activity of SMYD2 (data not shown). Furthermore, removing the first 13 amino acid residues from the S-sequence (SMYD2−dN1, Figure 1B, lane 5) also affected AdoMet binding, albeit to a lesser degree compared to the G18A/G20A double mutant (Figure 1C, column 5). The K_M of AdoMet for this mutant was increased by approximately 4-fold (0.12 ± 0.05 μM), whereas the V_{max} value remained unchanged. Consistent with our functional analysis, the X-ray crystal structure of SMYD2 showed that the S-sequence constitutes part of the AdoMet binding pocket, and the GxG motif makes direct electrostatic interactions with the methionine moiety of the AdoMet cosubstrate (Figure 5A).[40] Mutating residues G18 and G20 may impair the structural integrity of the AdoMet binding pocket, and thereby adversely affect AdoMet binding. Given the functional and structural importance of this region, it is not surprising that removing the first 13 residues affected AdoMet binding. Sirinupong et al. made a similar observation with SMYD1, where the S-sequence forms part of the AdoMet binding pocket, and a G18A/G20A mutant lost SMYD1 enzymatic activity.[36]

Functional Analysis of MYND, Post-SET, and CTD Domains. The MYND domain is a highly conserved zinc finger motif that mediates protein−protein interactions. It is found in a number of nuclear proteins such as AML1/ETO, Nervy, and DEAF-1, and has frequently been implicated in transcriptional repression.[37,38] Previous studies showed that deletion of the MYND domain had a negligible impact on the enzymatic activity of SMYD2.[17] This is consistent with the fact that the MYND domain packs around the SET domain on the opposite surface of the active site cleft and residues from the MYND domain do not contribute to the binding of either substrate.[36,40,41] To further assess the function of the MYND domain of SMYD2, we attempted to produce two mutants, C52A and C90A, in insect cells. Unfortunately, both mutants were insoluble, suggesting that these cysteine residues are important for the folding and stability of the SMYD2 protein. It remains to be addressed what is the functional significance of the MYND domain and what is the evolutionary driving force of incorporating such a zinc-finger domain in the SMYD protein family.

The functional importance of the post-SET domain in the SMYD family of proteins is poorly understood. In Dim-5, a cluster of four cysteine residues, three from the post-SET domain and one from the core SET domain, form a network that coordinates a zinc ion.[15] Sequence alignment suggested that a similar cysteine cluster

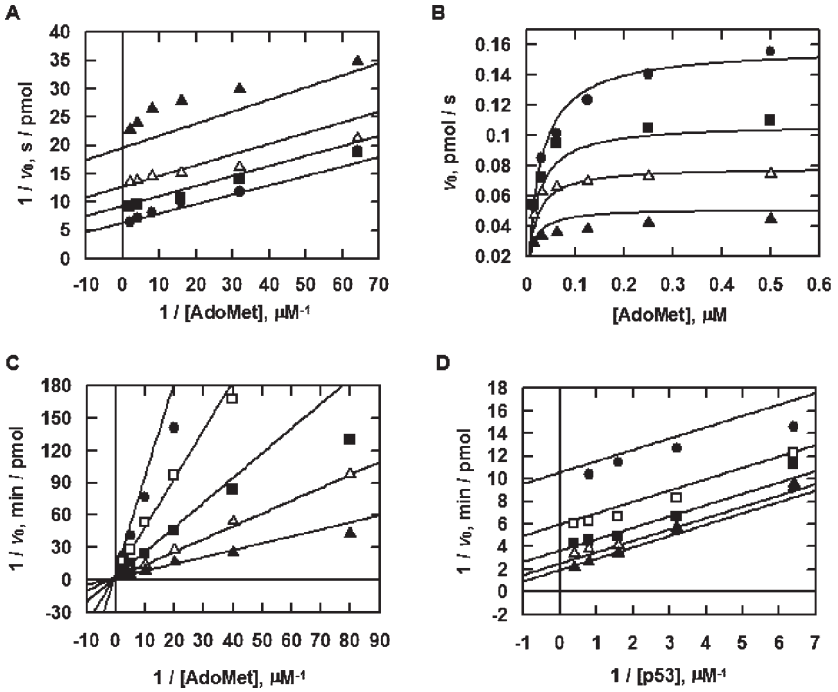

Figure 6. Kinetic analysis of SMYD2-catalyzed methylation of p53K370Me$_0$ peptide. See Experimental Procedures for details. (A) Double reciprocal plot of the methylation reaction initial velocities against AdoMet concentrations with several fixed concentrations of the p53K370Me$_0$ peptide: 0.25 μM (▲), 0.5 μM (△), 1 μM (■), and 4 μM (●). (B) Global fitting of untransformed data from (A) to a rapid equilibrium random Bi Bi model with eq 2. Solid lines represent the best fit. (C) Double reciprocal plot of the methylation reaction initial velocities against varying AdoMet concentrations and 1 μM p53K370Me$_0$ peptide substrate, and several fixed concentrations of AdoHcy: 0.78 μM (▲), 1.56 μM (△), 3.13 μM (■), 6.25 μM (□), and 12.5 μM (●). Solid lines represent the best fit of the data using eq 4. (D) Double reciprocal plot of the methylation reaction initial velocities against various p53K370Me$_0$ peptide concentrations with 0.5 μM AdoMet, and several fixed concentrations of AdoHcy: 0.78 μM (▲), 1.56 μM (△), 3.13 μM (■), 6.25 μM (□), and 12.5 μM (●). Solid lines represent the best fit of the data using eq 6.

could be formed from three cysteine residues (C262, C264, and C267) from the post-SET domain and one (C209) from the SET domain of SMYD2. Mutagenesis on the post-SET domain of SMYD2 indicated that this cluster of cysteine residues could participate in chelating a zinc ion, as its removal together with the CTD domain (SMYD2-dC3, M1-D256) reduced the zinc stoichiometry to two, whereas a truncation of the CTD domain alone (SMYD2-dC2, M1-K272) retained the zinc stoichiometry of three (Figure 4, right). Indeed, the X-ray crystal structure of SMYD2 revealed that these four cysteine residues coordinate a zinc ion (Figure 5B).[40] Similar zinc-binding post-SET cysteine clusters are also present in SMYD1 and SMYD3.[36,41] More importantly, the SMYD2 X-ray crystal structure clearly indicates that the zinc−cysteine complex in the post-SET domain helps maintain the structural integrity of SMYD2. Disrupting this region in SMYD2 reduced enzymatic activity. When C264 was mutated to alanine, the resulting mutant was found to have less than 10% activity compared to wild-type SMYD2. Complete removal of the post-SET domain (SMYD2-dC3) abolished SMYD2 activity (Figure 1C).

A highly conserved CTD domain is unique to the SMYD protein family. Recent structural work revealed that the SMYD family has an overall two-lobe structure. The first five domains (S-sequence, MYND, SET-I, core SET, and post-SET) form the N-terminal lobe and the CTD domain forms the C-terminal lobe. Interestingly, removing the CTD domain did not affect enzymatic activity as SMYD2-dC2 was fully active (Figure 1C). This is consistent with our structural work where we did not observe any significant motion of N- and C-lobes in the ternary complex with p53 peptide and AdoMet, and in the binary complex with AdoMet.[40] However, it was proposed that the CTD domain was involved in an autoinhibitory regulation mechanism and deletion or perturbation of the CTD domain enhanced SMYD1 activity.[36] More work needs to be done to establish the precise function of the CTD domain in the SMYD protein family.

Steady-State Analysis of SMYD2 Catalyzed Methylation of p53 Peptide. SMYD2-mediated methylation of p53 is predominantly a monomethylation event, thereby making it possible to evaluate the kinetic mechanism using classical bisubstrate kinetic models. To define the kinetic mechanism of SMYD2 catalysis, the AdoMet and p53K370Me$_0$ substrate concentrations were simultaneously varied at a range covering their respective K_M values. Figure 6B shows the untransformed data in which the initial velocity of the p53K370Me$_1$ product formation was determined by varying the AdoMet concentration with fixed concentrations of p53K370Me$_0$. The data was plotted in double-reciprocal format to visually inspect the kinetic mechanism. A series of apparently parallel lines were obtained from the reciprocal of either AdoMet or p53K370Me$_0$ concentration plotted against the reciprocal of velocity (Figure 6A). Parallel lines are usually indicative of either a Ping-Pong mechanism or a random sequential ternary complex mechanism under conditions of rapid equilibrium and large negative cooperativity between substrates.[42] To confirm the initial observations from the double-reciprocal plots, we globally fit the raw data to three typical kinetic models using GraFit with eqs 1−3. Close inspection of the results revealed that fitting to either random sequential Bi Bi (eq 2, Figure 6A, solid line) or Ping-Pong (eq 3, data not shown) model returned smaller ψ^2 values than fitting to an ordered sequential Bi Bi model (data not shown). The kinetic

Table 1. Steady-State Kinetic Parameters of SMYD2 as Determined by Global Fitting of the Initial Velocities of p53K370Me$_0$ Methylation Using eqs 1 and 3

	values	
kinetic constant	random ordered Bi Bi	Ping-Pong mechanism
k_{cat}	$0.048 \pm 0.001\ s^{-1}$	$0.048 \pm 0.001\ s^{-1}$
K_M, AdoMet	$0.031 \pm 0.010\ \mu M$[a]	$0.033 \pm 0.003\ \mu M$
K_M, p53 peptide	$0.68 \pm 0.22\ \mu M$[a]	$0.71 \pm 0.06\ \mu M$
α	11.7 ± 3.2	N/A

[a] K_Ms are calculated by multiplying the value of K_A (binding constant of AdoMet to EB complex) or K_B (binding constant of p53to EA complex) with the value of α.

constants obtained from these fittings are presented in Table 1. Global fitting of the data to random sequential Bi Bi and Ping-Pong models generated essentially identical kinetic parameters. Not surprisingly, the random sequential Bi Bi model also returned an α-value greater than one, indicating a negative cooperativity between these two substrates.

A Ping-Pong mechanism for PKMTs requires the formation of a methyl-PKMT intermediate. It is well established that PKMTs catalyze the lysine methylation via bimolecular nucleophilic substitution (S_N2) reactions, where the lysine side-chain amine acts as the nucleophile to directly attack the methyl leaving group on AdoMet.[39] Therefore a Ping-Pong mechanism could be ruled out as an option for SMYD2.

Kinetic Analysis of Product Inhibition. To confirm the mechanism of SMYD2-mediated methylation of the p53K370Me$_0$ substrate, the effect of the reaction product (AdoHcy) on catalysis was evaluated. Parts C and D of Figure 6 showed the effect of varying the AdoHcy concentration on the velocity of catalysis. In panel C, the concentration of p53K370Me$_0$ was used at its apparent K_M and the initial velocity was determined at varying concentrations of AdoMet and several fixed concentrations of AdoHcy. The untransformed data was fit to the Michaelis−Menten equation (eq 4) at each inhibitor (AdoHcy) concentration, and the calculated kinetic parameters were used to generate a double-reciprocal plot. These results showed a series of lines that converge at the *y*-axis of the double-reciprocal plot, as expected for a competitive inhibitor (Figure 6C). Global fitting of the untransformed data from this experiment to eq 4 for competitive inhibition yielded a K_I of $0.35 \pm 0.001\ \mu M$ for AdoHcy. In Figure 6D, the reaction was studied at varying p53K370Me$_0$ substrate concentrations and several fixed concentrations of AdoHcy, with the AdoMet concentration held constant at its apparent K_M. These data were analyzed as described above, and produced a series of parallel lines in the double-reciprocal plot, consistent with AdoHcy being an uncompetitive inhibitor with respect to the p53K370Me$_0$ substrate.

Although parallel double-reciprocal lines suggest a Ping-Pong mechanism, a classical Ping-Pong mechanism requires that the reaction product be noncompetitive with its cognate substrate (AdoMet) and competitive with the second substrate of the enzyme (p53K370Me$_0$).[42] We observed a different AdoHcy inhibition pattern (competitive with AdoMet and uncompetitive with the p53K370Me$_0$), further suggesting that SMYD2 catalysis does not follow a Ping-Pong mechanism. The product of bisubstrate reactions following a random sequential Bi Bi mechanism is normally a competitive inhibitor to its cognate substrate and a noncompetitive inhibitor to the other substrate. However, according to Segal,[42] the product could appear to be uncompetitive to the other substrate when the product does not inhibit the binding of its cognate substrate strongly. The K_I of AdoHcy was determined to be around 350 nM, almost ten times higher than the K_M of AdoMet, making it a weak inhibitor of AdoMet. Therefore, it is not surprising to observe AdoHcy being uncompetitive to p53K370Me$_0$ even though SMYD2 catalysis adopts a random sequential Bi Bi mechanism under rapid equilibrium conditions.

CONCLUSIONS

Here we present the expression, purification, and characterization of human SMYD2, and show that it methylates histones H2B, H3.2, H4, and the nonhistone protein p53. We also confirmed by LC-MS that SMYD2 monomethylates the p53K370Me$_0$ peptide. SMYD2 methyltransferase activity is pH-dependent and is maximal at pH values greater than nine. Furthermore, SMYD2 was shown to contain three tightly bound zinc ions based on our PAR/PMB biochemical assay and ICP-MS analysis.

The SMYD protein family has a unique split SET domain (Figure 1). We have now firmly established that the S-sequence that contains the GxG motif in the split SET domain is important for optimal enzymatic activity. We established that the cysteine-rich post-SET domain was essential for enzymatic activity, as removing this domain abolished enzymatic activity completely. However, the CTD domain that lies after the post-SET domain seems to be dispensable for the enzymatic activity of SMYD2 in our biochemical assay system when p53K370Me$_0$ was used as substrate, as we did not observe any noticeable difference in specific SMYD2 enzymatic activity when the CTD domain was deleted.

Similar to other SET domain-containing PKMTs, SMYD2 catalyzes the methylation of the p53K370Me$_0$ substrate via a random sequential Bi Bi mechanism under rapid equilibrium conditions as evidenced by both steady-state kinetic analysis and product inhibition studies. This kinetic mechanism impacts the design and characterization of inhibitors for enzymes with multiple substrates. The random sequential Bi Bi mechanism that SMYD2 adopts suggests that we should have a nonbiased screening assay irrespective of the sequence of reagent addition.

To our knowledge, this study represents the first kinetic study of a PKMT using a nonhistone peptide substrate and the first detailed biochemical characterization of a member of the SMYD protein family, which has a unique domain arrangement. Methylation of lysines on nonhistone proteins has emerged as an important post-translational modification for the functional regulation of proteins involved in cell signaling transduction, cell apoptosis, and cell cycle control. The results presented in this study further the mechanistic understanding of the SMYD2 catalyzed methyl group transfer reaction and the functional importance of distinct SMYD2 domains. This work should lay the foundation for designing robust biochemical assays for identifying SMYD2 small molecule inhibitors that may serve as a useful pharmacological tool for mechanistic and functional studies in cells.

AUTHOR INFORMATION

Corresponding Author

*For J.W.: phone, 781-839-4077; fax, 781-839-4200; E-mail, jiaquan.wu@astrazeneca.com. For H.C.: phone, 781-839-4417; Fax, 781-839-4200; E-mail: raymond.chen@astrazeneca.com.

Author Contributions

§These authors contributed equally to this work.

■ ACKNOWLEDGMENT

We are grateful to members of the Oncology Biochemistry group and Dr. Nicholas Larsen at AstraZeneca R&D Boston for material support and data discussion. We thank Dr. Stewart Fisher for critical reading of the manuscript and data discussion, Dr. Daniel Russell for the initial SMYD2 structure homology modeling, and Hannah Pollard and Dr. Isabelle Green for providing SMYD2 truncation mutant proteins.

■ ABBREVIATIONS USED

AdoHcy, *S*-adenosylhomocysteine; AdoMet, *S*-adenosylmethionine; CTD, C-terminal domain; ICP-MS, inductively coupled plasma mass spectrometry; MYND, Myeloid, Nervy and DEAF-1; PAR, 4-(2-pyridylazo)-resorcinol; PKMT, protein lysine methyltransferase; PMB, *p*-(hydroxymercuri)-benzoic acid; SET, Su(var.)3−9, En(zeste), Trithorax; SMYD, SET- and MYND-domain containing protein; SPA, scintillation proximity assay

■ REFERENCES

(1) Martin, C., and Zhang, Y. (2005) The diverse functions of histone lysine methylation. *Nature Rev. Mol. Cell Biol. 6*, 838–849.

(2) Shi, Y. (2007) Histone lysine demethylases: emerging roles in development, physiology and disease. *Nature Rev. Genet. 8*, 829–833.

(3) Bannister, A. J., and Kouzarides, T. (2005) Reversing histone methylation. *Nature 436*, 1103–1106.

(4) Kubicek, S., and Jenuwein, T. (2004) A crack in histone lysine methylation. *Cell 119*, 903–906.

(5) Scoumanne, A., and Chen, X. (2008) Protein methylation: a new mechanism of p53 tumor suppressor regulation. *Histol. Histopathol. 23*, 1143–1149.

(6) Kurash, J. K., Lei, H., Shen, Q., Marston, W. L., Granda, B. W., Fan, H., Wall, D., Li, E., and Gaudet, F. (2008) Methylation of p53 by Set7/9 mediates p53 acetylation and activity in vivo. *Mol. Cell 29*, 392–400.

(7) Huang, J., Perez-Burgos, L., Placek, B. J., Sengupta, R., Richter, M., Dorsey, J. A., Kubicek, S., Opravil, S., Jenuwein, T., and Berger, S. L. (2006) Repression of p53 activity by Smyd2-mediated methylation. *Nature 444*, 629–632.

(8) Saddic, L. A., West, L. E., Aslanian, A., Yates, J. R., III, Rubin, S. M., Gozani, O., and Sage, J. (2010) Methylation of the retinoblastoma tumor suppressor by SMYD2. *J. Biol. Chem. 285*, 37733–37740.

(9) Kontaki, H., and Talianidis, I. (2010) Lysine methylation regulates E2F1-induced cell death. *Mol. Cell 39*, 152–160.

(10) Yang, X. D., Tajkhorshid, E., and Chen, L. F. (2010) Functional interplay between acetylation and methylation of the RelA subunit of NF-kappaB. *Mol. Cell. Biol. 30*, 2170–2180.

(11) Lu, T., Jackson, M. W., Wang, B., Yang, M., Chance, M. R., Miyagi, M., Gudkov, A. V., and Stark, G. R. (2010) Regulation of NF-kappaB by NSD1/FBXL11-dependent reversible lysine methylation of p65. *Proc. Natl. Acad. Sci. U.S.A. 107*, 46–51.

(12) Kunizaki, M., Hamamoto, R., Silva, F. P., Yamaguchi, K., Nagayasu, T., Shibuya, M., Nakamura, Y., and Furukawa, Y. (2007) The Lysine 831 of Vascular Endothelial Growth Factor Receptor 1 Is a Novel Target of Methylation by SMYD3. *Cancer Res. 67*, 10759–10765.

(13) Esteve, P. O., Chin, H. G., Benner, J., Feehery, G. R., Samaranayake, M., Horwitz, G. A., Jacobsen, S. E., and Pradhan, S. (2009) Regulation of DNMT1 stability through SET7-mediated lysine methylation in mammalian cells. *Proc. Natl. Acad. Sci. U.S.A. 106*, 5076–5081.

(14) Barski, A., Cuddapah, S., Cui, K., Roh, T. Y., Schones, D. E., Wang, Z., Wei, G., Chepelev, I., and Zhao, K. (2007) High-resolution profiling of histone methylations in the human genome. *Cell 129*, 823–837.

(15) Cheng, X., Collins, R. E., and Zhang, X. (2005) Structural and sequence motifs of protein (histone) methylation enzymes. *Annu. Rev. Biophys. Biomol. Struct. 34*, 267–294.

(16) Brown, M. A., Sims, R. J.,III, Gottlieb, P. D., and Tucker, P. W. (2006) Identification and characterization of Smyd2: A split SET/MYND domain-containing histone H3 lysine 36-specific methyltransferase that interacts with the Sin3 histone deacetylase complex. *Mol. Cancer 5*, 1–11.

(17) Abu-Farha, M., Lambert, J., Al-Madhoun, A. S., Elisma, F., Skerjanc, I. S., and Figeys, D. (2008) The tale of two domains: proteomics and genomics analysis of SMYD2, a new histone methyltransferase. *Mol. Cell. Proteomics 7*, 560–572.

(18) Silva, F. P., Hamamoto, R., Kunizaki, M., Tsuge, M., Nakamura, Y., and Furukawa, Y. (2008) Enhanced methyltransferase activity of SMYD3 by the cleavage of its N-terminal region in human cancer cells. *Oncogene 27*, 2686–2692.

(19) Chang, Y., Zhang, X., Horton, J. R., Upadhyay, A. K., Spannhoff, A., Liu, J., Snyder, J. P., Bedford, M. T., and Cheng, X. (2009) Structural basis for G9a-like protein lysine methyltransferase inhibition by BIX-01294. *Nature Struct. Mol. Biol. 16*, 312–317.

(20) Zhang, X., Yang, Z., Khan, S. I., Horton, J. R., Tamaru, H., Selker, E. U., and Cheng, X. (2003) Structural basis for the product specificity of histone lysine methyltransferases. *Mol. Cell 12*, 177–185.

(21) Patnaik, D., Chin, H. G., Esteve, P. O., Benner, J., Jacobsen, S. E., and Pradhan, S. (2004) Substrate specificity and kinetic mechanism of mammalian G9a histone H3 methyltransferase. *J. Biol. Chem. 279*, 53248–53258.

(22) Obianyo, O., Osborne, T. C., and Thompson, P. R. (2008) Kinetic mechanism of protein arginine methyltransferase 1. *Biochemistry 47*, 10420–10427.

(23) Baron, R. A., and Casey, P. J. (2004) Analysis of the kinetic mechanism of recombinant human isoprenylcysteine carboxylmethyltransferase (Icmt). *BMC Biochem. 5*, 19.

(24) Rooney, P. H., Murray, G. I., Stevenson, D. A., Haites, N. E., Cassidy, J., and McLeod, H. L. (1999) Comparative genomic hybridization and chromosomal instability in solid tumours. *Br. J. Cancer 80*, 862–873.

(25) Komatsu, S., Imoto, I., Tsuda, H., Kozaki, K. I., Muramatsu, T., Shimada, Y., Aiko, S., Yoshizumi, Y., Ichikawa, D., Otsuji, E., and Inazawa, J. (2009) Overexpression of SMYD2 relates to tumor cell proliferation and malignant outcome of esophageal squamous cell carcinoma. *Carcinogenesis 30*, 1139–1146.

(26) Hamamoto, R., Silva, F. P., Tsuge, M., Nishidate, T., Katagiri, T., Nakamura, Y., and Furukawa, Y. (2006) Enhanced SMYD3 expression is essential for the growth of breast cancer cells. *Cancer Sci. 97*, 113–118.

(27) Zamble, D. B., McClure, C. P., Penner-Hahn, J. E., and Walsh, C. T. (2000) The McbB component of microcin B17 synthetase is a zinc metalloprotein. *Biochemistry 39*, 16190–16199.

(28) Hunt, J. B., Neece, S. H., and Ginsburg, A. (1985) The use of 4-(2-pyridylazo)resorcinol in studies of zinc release from *Escherichia coli* aspartate transcarbamoylase. *Anal. Biochem. 146*, 150–157.

(29) Changeux, J. P., Gerhart, J. C., and Schachman, H. K. (1968) Allosteric interactions in aspartate transcarbamylase. I. Binding of specific ligands to the native enzyme and its isolated subunits. *Biochemistry 7*, 531–538.

(30) Subramani, S., and Schachman, H. K. (1981) The mechanism of dissociation of aspartate transcarbamoylase by *p*-mercuribenzoate. *J. Biol. Chem. 256*, 1255–1262.

(31) Cook, P. F., and Cleland, W. W. (2007) *Enzyme Kinetics and Mechanism*; p 416, Garland Sciences, New York.

(32) Zhang, X., and Bruice, T. C. (2008) Enzymatic mechanism and product specificity of SET-domain protein lysine methyltransferases. *Proc. Natl. Acad. Sci. U.S.A. 105*, 5728–5732.

(33) Dirk, L. M. A., Flynn, E. M., Dietzel, K., Couture, J., Trievel, R. C., and Houtz, R. L. (2007) Kinetic manifest of processivity during multiple methylation catalyzed by SET domain protein methyltransferase. *Biochemistry 46*, 3905–3915.

(34) Zhang, X., Tamaru, H., Khan, S. I., Horton, J. R., Keefe, L. J., Selker, E. U., and Cheng, X. (2002) Structure of the Neurospora SET domain protein DIM-5, a histone H3 lysine methyltransferase. *Cell 111*, 117–127.

(35) Boyer, P. D. (1954) Spectrophotometric study of the reaction of protein sulfhydryl groups with organic mercurials. *J. Am. Chem. Soc. 76*, 4331–4337.

(36) Sirinupong, N., Brunzelle, J., Ye, J., Pirzada, A., Nico, L., and Yang, Z. (2010) Crystal structure of cardiac-specific histone methyltransferase SmyD1 reveals unusual active site architecture. *J. Biol. Chem. 285*, 40635–40644.

(37) Liu, Y., Chen, W., Gaudet, J., Cheney, M. D., Roudaia, L., Cierpicki, T., Klet, R. C., Hartman, K., Laue, T. M., Speck, N. A., and Bushweller, J. H. (2007) Structural basis for recognition of SMRT/N-CoR by the MYND domain and its contribution to AML1/ETO's activity. *Cancer Cell. 11*, 483–497.

(38) Barth, S., Edlich, F., Berchner-Pfannschmidt, U., Gneuss, S., Jahreis, G., Hasgall, P. A., Fandrey, J., Wenger, R. H., and Camenisch, G. (2009) Hypoxia-inducible factor prolyl-4-hydroxylase PHD2 protein abundance depends on integral membrane anchoring of FKBP38. *J. Biol. Chem. 284*, 23046–23058.

(39) Copeland, R. A., Solomon, M. E., and Richon, V. M. (2009) Protein methyltransferases as a target class for drug discovery. *Nature Rev. Drug Discovery 8*, 724–732.

(40) Ferguson, A. D., Larsen, N. A., Howard, T., Pollard, H., Green, I., Grande, C., Cheung, T., Garcia-Arenas, R., Cowen, S., Wu, J., Godin, R., Chen, H., and Keen, N. (2011) Structural Basis of Non-Histone Substrate Methylation and Selective Inhibition of SMYD2. *Structure* in press.

(41) Sirinupong, N., Brunzelle, J., Doko, E., and Yang, Z. (2011) Structural insights into the autoinhibition and posttranslational activation of histone methyltransferase SmyD3. *J. Mol. Biol. 406*, 149–159.

(42) Segel, I. H. (1993) *Enzyme Kinetics: Behavior and Analysis of Rapid Equilibrium and Steady-State Enzyme Systems*; Wiley Classics Library, New York.